Reactions in clusters

Harri-Pekka Kaukonen,[a] Uzi Landman, and C. L. Cleveland
School of Physics, Georgia Institute of Technology, Atlanta, Georgia 30332

(Received 11 March 1991; accepted 4 June 1991)

A new class of cluster-catalyzed reactions is proposed and investigated using extensive molecular-dynamics simulations. These reactions involve the collision between reactants which are embedded in inert gas clusters, whose role is that of a local heat bath (i.e., extended third body). The concept is demonstrated for the reactions $[Na_4Cl_3]^+Ar_q + Cl^-$ (for $q = 12$ and 32) and $[Na_{14}Cl_{12}]^{+2}Ar_{30} + Cl^-$ for several initial temperatures, relative translational energies between the reactants, and impact parameters. For associative reactions, i.e., Cl^- attachment accompanied by the release of Ar atoms, the dynamics of the reactions, the dependencies of the isomeric structures of the product alkali-halide clusters, and of reaction pathways and branching ratios on reactant size and reaction conditions are systematically studied.

I. INTRODUCTION

Small materials aggregates (clusters) often exhibit thermodynamic, structural, energetic, dynamic, electronic, and chemical properties which differ from those of bulk materials, reflecting the finite-size of these systems. Much progress has been achieved in the experimental[1] generation, size selection, characterization, and probing of the properties of clusters, and in the theoretical treatment of finite systems in both the classical[2] and quantum regimes.[3] However, relatively few investigations of the chemical properties of cluster systems, and in particular chemical reactions between colliding clusters or clusters colliding with atomic, molecular, or ionic reactants, have been made.[4,5] In this context we note studies of the reactivity of metallic clusters, catalyzing dissociation of small molecules (H_2, D_2, and O_2), and the correlations which have been deduced between the chemical activity and variations in electronic and structural properties of clusters of different sizes (variable number of particles).

In this paper we propose and demonstrate a new mode, of nonelectronic nature, by which clusters may catalyze reactions (CCR). In this mode reactants are embedded in colliding clusters and the role of the cluster environment is that of a local heat bath (i.e., extended third body). The purpose of our study is to demonstrate such reactions, using classical molecular dynamics (MD) simulations for model systems, and to illustrate ways by which reaction pathways and branching ratios may be controlled by the cluster environment.

We emphasize that while issues concerning the kinetics and energetics of cluster formation and of solvation in clusters under various conditions have been the subject of a number of investigations,[1,6,7] our focus is on reactions involving preformed clusters where one (or both) of the reactants are embedded in the cluster(s). In addition to this main subject, our studies may relate to certain issues pertaining to the dynamics and kinetics of gas-phase recombination processes (particularly ion–ion recombination). While a theoretical framework for treating termolecular ion–ion recombination ($A^+ + B^- + M \rightarrow AB + M$, where A^+ and B^- are reactants and M is a gas of a given density) has been formulated,[8,9] where the effect of a multistep series of stochastic collisions of a A^+–B^- pair with the gas molecules (M) is included, effects due to clustering of gas molecules about the reactant ions have not been incorporated. Indeed, a recent assessment[9] of the current status of research in this area concludes with regard to ion–ion recombination that "there are at present no measurements from a given laboratory which span the full range of gas pressures studied theoretically and which monitor the identity of ions as the pressure changes. The task is difficult in that the ions may well be clustered to high orders." In this respect, the studies presented in this paper may provide the impetus for the incorporation of clustering effects in theoretical treatments of the kinetics and dynamics of ion–ion recombination at high inert-gas ambient pressure.

The method and systems used in our studies are described in Sec. II, followed by our results given in Sec. III. We conclude in Sec. IV, summarizing our results and proposing future directions.

II. METHOD AND SYSTEMS

The reaction systems that we have chosen to investigate are mixed clusters composed of small charged sodium-chloride fragments embedded in argon, colliding with a Cl^- anion. To investigate the dependence on size, several reaction systems were investigated: (i) $[Na_4Cl_3]^+Ar_q$ for $q = 12$ and 32 and (ii) $[Na_{14}Cl_{12}]^{+2}Ar_{30}$. Furthermore, systematic dependencies on characteristic parameters of the reaction were studied (i.e., initial temperature of the cluster, relative translational kinetic energy between the collision partners, and impact parameters).

The interactions between the ionic constituents are described in our studies by Coulomb and Born–Meyer repulsion potentials, parametrized according to Born and Huang.[10] For the interaction between the argon atoms and the Na^+ and Cl^- ions, the potentials developed by Ahrlrichs *et al.*[11] were used.

[a] Permanent address: Laboratory of Physics, Helsinki University of Technology 02150 Espoo, Finland.

Given these interaction potentials, we have performed extensive MD simulations, where the classical particles' equations of motion (in the center of mass coordinate frame) were solved using Gear's fifth-order predictor–corrector algorithm,[12] with an integration time step $\Delta t = 1.03 \times 10^{-15}$ s. Prior to collision the isolated clusters were equilibrated using the stochastic collision method.[13] For each choice of reaction parameters 100 collisions were run with the impact parameters r_I, between the Cl^- and the center of mass of the target cluster, sampled according to

$$r_I = 2R_{\max}\sqrt{s}, \tag{1}$$

where s is a random number in the interval [0,1], and $R_{\max}$ is an estimate of the radius of the target cluster [$R_{\max} = 4$ Å for the systems in (i) and 4.8 Å for the larger system in (ii)]. This sampling procedure yields random uniform coverage of the cross-sectional area of the target clusters. The mean impact parameter is given by $\bar{r}_I = 4R_{\max}/3$.

In summary, the simulation procedure which we used is as follows:

(a) First, 50 uncorrelated equilibrium configurations of the target cluster, selected out of the equilibrium ensemble, were stored;

(b) for each study, 100 reaction trajectories were simulated, where in each case a cluster configuration was randomly chosen from the above set of equilibrium configurations, to which a random rotation was applied. Finally, the impact parameters between the clusters and the Cl^- were selected randomly according to Eq. (1). The initial distance between the reactants was 32 Å in each case.

The results, which we present in Sec. III, are averaged in each case over the 100 simulated trajectories.

III. RESULTS

The two sodium-chloride systems which we investigated, are characterized by their enhanced stability, reflected in cluster beam abundance spectra, which is associated with the cuboid structure of the products Na_4Cl_4 and $[Na_{14}Cl_{13}]^+$ in their lowest energy states.[14] However, clusters are known to exhibit a sequence of structural isomers, between which they transform upon heating.[2,14]

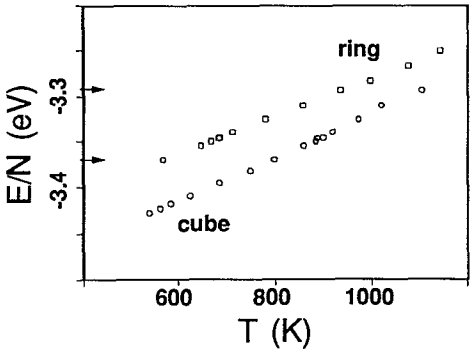

FIG. 1. Caloric curve (total energy per particle, E/N, vs kinetic temperature, T) calculated for Na_4Cl_4. The energy region between the arrows on the E axis correspond to the coexistence region. Energy in units of eV and temperature in K.

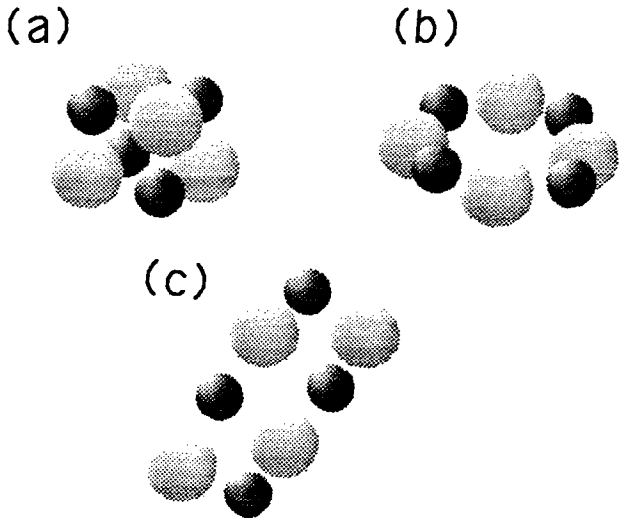

FIG. 2. Structures of the ground state isomer [in (a)] and next-higher isomer [in (b)] of Na_4Cl_4 selected from finite-temperature simulations. Also, we show the next-in-energy (ladder) isomer through which the cluster transforms between the cube and ring structures. Dark and light spheres represent Na^+ and Cl^- ions, respectively.

The cluster structural isomerization can be investigated via the caloric relationship, i.e., total energy of the system vs kinetic temperature (defined as $T = 2\langle E_k \rangle / k_B(3N-6)$, where $\langle E_k \rangle$ is the average kinetic energy of the system, $3N-6$ is the number of degrees of freedom for a stationary nonrotating cluster of N particles, and k_B is Boltzmann's constant). The caloric curve for Na_4Cl_4 shown in Fig. 1 exhibits two branches.[14(c)] The data in the figure was obtained via constant energy simulations (microcanonical ensemble). Upon heating the system for temperatures $T \lesssim 800$ K, the system is found only in the cubic structure [see Fig. 2(a)]. Systems with a larger total energy content exhibit transformations between the ground state cubic isomer and the next-higher one which possesses a ring structure[14(c)] [see Fig. 2(b)]. The total per-particle energy range -3.37 eV $\lesssim E \lesssim -3.29$ eV is characterized as a coexistence region where the cluster fluctuates between the two isomers. The data in this region was calculated by averaging separately over time regions in which the cluster was found in a particular isomeric form. [Typical simulations times in the coexistence region were $\sim (5\text{–}10) \times 10^6\, \Delta t$.] For clusters with energy content above the upper limit of the coexistence region (i.e., $E \gtrsim -3.29$ eV), only the ring isomeric form is found.

The larger cluster $[Na_{14}Cl_{13}]^+$, which in the ground state is a $3 \times 3 \times 3$ filled cuboid (with three ions of alternating charges on an edge), possesses a number of structural isomers (the same applies to the $[Na_{14}Cl_{12}]^{+2}$ cluster, where in the ground state cuboid isomer the central Cl^- anion is missing). The structures of the $[Na_{14}Cl_3]^+$ and $[Na_{14}Cl_{12}]^{+2}$ collision partners, in the argon cluster environments (equilibrated at $T = 31.6$ K), are shown in Fig. 3.

Upon collision of a Cl^- with a $[Na_nCl_m]^{+(n-m)}Ar_q$ cluster, a fraction of the relative translational kinetic energy between the collision partners, as well as the binding energy

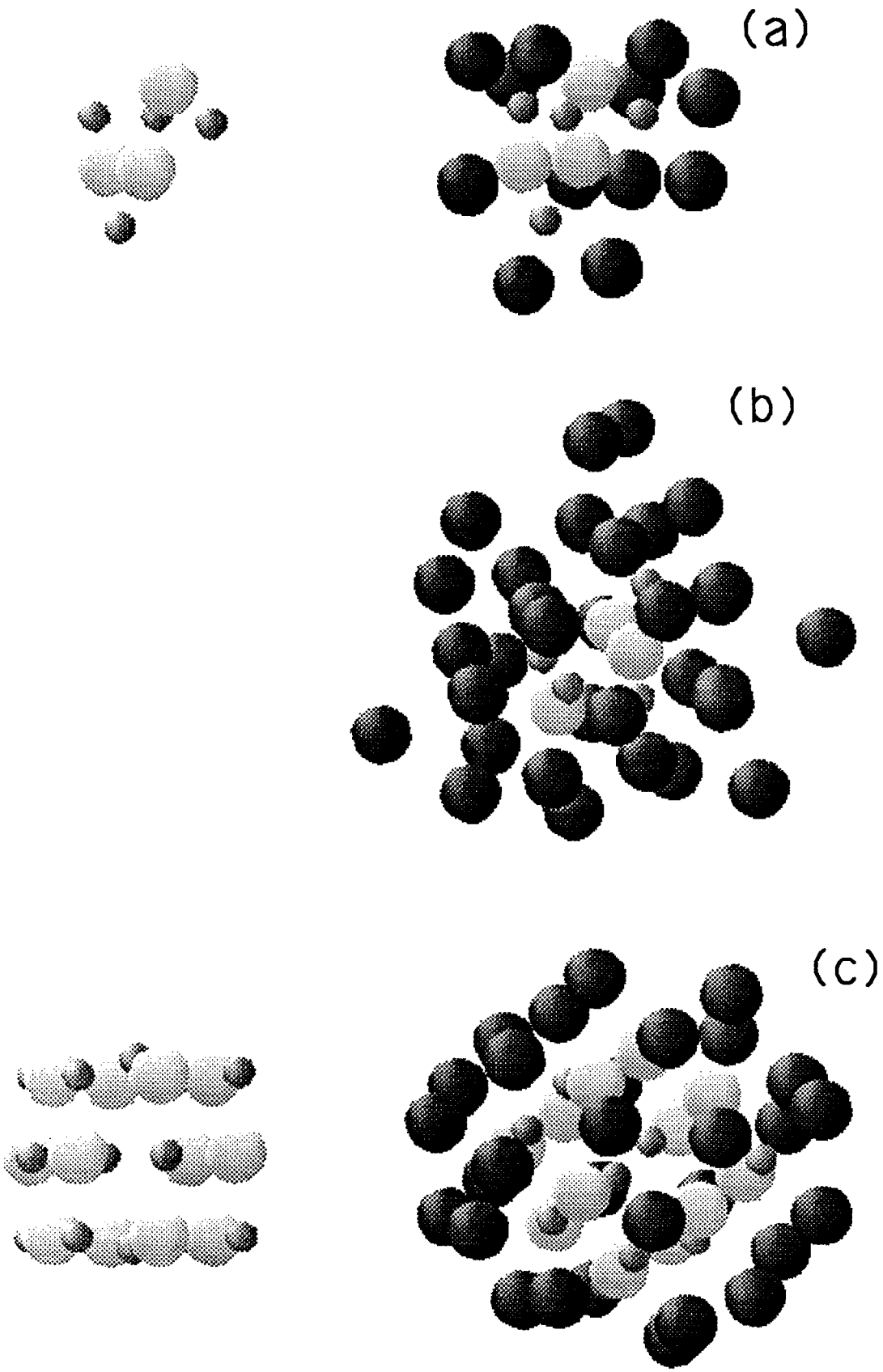

FIG. 3. Selected equilibrium configurations at a vibrational temperature $T^0_{vib} = 31.6$ K of charged sodium-chloride clusters, embedded in argon environments. The configurations were obtained during the preparation stage prior to collision with Cl^-. In (a) and (b) the structures of $[Na_4Cl_3]^+Ar_{12}$ and $[Na_4Cl_3]^+Ar_{32}$ are shown, respectively. Additionally, we show in (a) the structure of $[Na_4Cl_3]^+$ with the Ar atoms removed. The structure of $[Na_{14}Cl_{12}]^{+2}Ar_{30}$ (with and without the Ar atoms) is shown in (c). Dark spheres represent Ar atoms; light large spheres and grey small ones represent Cl^- and Na^+ ions.

released upon reaction, is imparted to the compound (combined) cluster (i.e., the intermediate cluster composed of the two colliding entities). Since the binding energies between the Ar atoms, and between them and the alkali-halide ions are significantly smaller than the binding energy between the Na^+ and Cl^- ions, the released excess energy could result in breaking of argon atom bonds to the cluster. Consequently, we would expect that the heat content of the combined, collision-intermediate cluster will be reduced via ejection of Ar atoms, resulting in effective cooling of the products. Under ideal circumstances (which depend on system parameters, such as activation barriers, binding strengths, vibrational relaxation times, initial temperature, and relative translational energy), one could expect that such a process may anneal the product to its lowest (ground) state (in our particular example, to the low-temperature cubic isomer).

In light of the above discussion, we present in this section the results of our simulations; first for $[Na_4Cl_3]^+Ar_q + Cl^-$ ($q = 12$ and 32), followed by results for the $[Na_{14},Cl_{12}]^{+2}Ar_{30} + Cl^-$ reaction system.

A. $[Na_4Cl_3]^+Ar_q + Cl^-$

1. Product distributions

As we discussed above, the reaction of $[Na_4Cl_3]^+Ar_q$ with Cl^- may lead to the formation of $[Na_4Cl_4]Ar_{q'}$ ($0 \leqslant q' \leqslant q$). Three systems have been studied with initial $q = 0$, 12, and 32. In this subsection we focus on reactions which results in the above products. Collision events leading to other products are discussed separately.

First we note that the reaction of Cl^- with bare charged $[Na_4Cl_3]^+$ clusters (i.e., $q = 0$) results in fragmentation or high-potential-energy isomers (open chains), even for vanishingly small initial relative translational kinetic energy, E_R.

Results (averaged in each case over 100 collision trajectories, each lasting for 25 ps after impact between the collision partners defined from the time when the distance between the Cl^- and any atom in the target cluster is less than a cutoff distance of 7.9 Å) for the reactions with $q = 12$ are shown in Tables I and II for two collision conditions: (i)

TABLE I. (a) Averaged results (over 100 trajectories in each case) for the reaction $[Na_4Cl_3]^+Ar_{12} + Cl$ with the initial target clusters selected from an equilibrium ensemble at $T^0_{vib} = 31.6$ K. Data is given for collisions resulting in cube- and ring-isomeric products $[Na_4Cl_4]Ar_{q'}$ for different values of the initial relative translational energy between the reactants (E_R, cases I to V). For each case the values in the first row are for cube-isomer products and those in parenthesis are for ring-isomer products. For both product forms the values in the row under the mean values are the standard deviations from the mean. Large standard deviations in some of the quantities given in this table, as well as in other tables, reflect mainly broad distributions rather than statistical errors. The initial energy of the system is denoted by E^0 and the relative translational energy between the reactants by E_R. P_C and P_R are the probabilities for formation of cube or ring isomers, respectively. $P_C + P_R$ is the total probability of reaction, and P_C/P_R the relative probabilities. N_f is the average number of atoms in the product mixed cluster and r_f is the average impact parameter. The total final, potential, vibrational, rotational, and translational energies of the product mixed clusters are denoted by E_f, E_p, E_{vib}, E_{rot}, and E_{tr}, and their average temperature by T_{vib}. Energies in eV, temperatures in degrees Kelvin and the impact parameters in Å. The two cases at the bottom of the table correspond to those collision events (with initial conditions as in case IV) which lead to reaction products $[Na_3Cl_3]Ar_q + NaCl$, (denoted as case IV, dimer) or glancing collisions (denoted as case IV, glancing). The values under the P_C column correspond to the probabilities of these events. For both cases the first row gives the mean values and the one under it the standard deviation from the mean. (b) Same as (a) for the reaction $[Na_4Cl_3]^+Ar_{12} + Cl$ with the initial target clusters selected from an equilibrium ensemble at $T^0_{vib} = 189$ K. Cases I to V correspond to different values of initial relative translational energy between the reactions, E_R. Energies in eV, temperatures in degrees Kelvin, and the impact parameters in Å. (c) Same as (a) for the reaction $[Na_4Cl_3]^+Ar_{12} + Cl$ with the initial target clusters selected from an equilibrium ensemble at $T^0_{vib} = 316$ K. Cases I to IV correspond to different values of initial relative translational energy between the reactants, E_R. Energies in eV, temperatures in degrees Kelvin, and the impact parameters in Å.

(a) Case	T_{vib}	E_{vib}	E_{rot}	E_{tr}	E_p	E_f	r_f	N_f	E^0	E_R	$P_{C(R)}$	$P_C + P_R$	P_C/P_R
I	480	0.74	0.052	0.067	−29.65	−28.79	5.82	13.6	−27.51	0.	0.46	1.0	0.85
	57	0.11	0.032	0.040	0.60	0.40	1.82	1.4	0.01				
	(515)	(0.75)	(0.047)	(0.042)	(−29.27)	(−28.43)	(5.50)	(13.0)	(−27.51)		(0.54)		
	76	0.14	0.035	0.027	0.55	0.35	2.02	1.3	0.01				
II	480	0.73	0.043	0.077	−29.41	−28.57	5.30	13.4	−27.10	0.41	0.40	1.0	0.67
	54	0.12	0.030	0.064	0.68	0.46	1.67	1.7	0.01				
	(515)	(0.72)	(0.054)	(0.068)	(−29.14)	(−28.30)	(5.24)	(12.6)	(−27.10)		(0.60)		
	69	0.11	0.051	0.040	0.61	0.41	2.05	1.4	0.01				
III	480	0.72	0.052	0.109	−29.67	−28.79	4.92	13.5	−26.44	1.08	0.42	0.98	0.75
	80	0.11	0.047	0.060	0.92	0.70	1.81	2.0	0.01				
	(536)	(0.71)	(0.054)	(0.092)	(−28.97)	(−28.11)	(4.87)	(12.1)	(−26.44)		(0.56)		
	76	0.10	0.036	0.050	0.69	0.50	2.03	1.5	0.01				
IV	502	0.69	0.051	0.099	−29.30	−28.46	4.39	12.6	−25.61	1.90	0.27	0.82	0.49
	82	0.12	0.037	0.058	0.75	0.54	1.80	1.8	0.01				
	(606)	(0.72)	(0.060)	(0.100)	(−28.55)	(−27.67)	(5.68)	(11.0)	(−25.60)		(0.55)		
	120	0.10	0.040	0.060	0.90	0.68	1.53	1.9	0.01				
V	496	0.72	0.052	0.270	−29.61	−28.57	3.86	13.4	−22.99	4.52	0.09	0.44	0.26
	66	0.15	0.049	0.118	1.10	0.78	0.90	2.7	0.01				
	(688)	(0.71)	(0.079)	(0.171)	(−28.20)	(−27.24)	(4.23)	(10.3)	(−22.99)		(0.35)		
	246	0.16	0.063	0.085	1.30	1.01	1.62	2.2	0.01				
IV	417	0.52	0.043	0.140	−23.01	−22.31	6.42	14.6	−25.60	1.90	0.08		
Dimer	196	0.06	0.027	0.080	0.49	0.33	1.75	1.4	0.01				
IV	234	0.50	0.024	0.026	−26.60	−26.04	7.32	18.8	−25.60	1.90	0.10		
Glancing	63	0.14	0.016	0.016	0.47	0.30	0.42	0.4	0.01				

TABLE I. (*Continued.*)

(b)

Case	T_{vib}	E_{vib}	E_{rot}	E_{tr}	E_p	E_f	r_I	N_f	E^0	E_R	$P_{C(R)}$	P_C+P_R	P_C/P_R
I	531	0.72	0.047	0.069	−29.15	−28.31	5.49	12.3	−26.74	0.	0.38	1.0	0.61
	70	0.09	0.036	0.040	0.57	0.40	1.90	1.2	0.07				
	(578)	(0.72)	(0.049)	(0.059)	(−28.66)	(−27.83)	(5.23)	(11.3)	(−26.74)		(0.62)		
	66	0.11	0.038	0.049	0.52	0.32	1.75	1.1	0.04				
II	556	0.73	0.046	0.074	−29.04	−28.19	5.64	12.0	−26.45	0.30	0.30	0.99	0.43
	82	0.14	0.044	0.039	0.71	0.49	1.75	1.5	0.04				
	(581)	(0.72)	(0.050)	(0.057)	(−28.68)	(−27.85)	(5.33)	(11.4)	(−26.44)		(0.69)		
	79	0.10	0.032	0.051	0.60	0.41	1.68	1.2	0.04				
III	540	0.70	0.048	0.104	−29.08	−28.23	5.27	12.0	−26.02	0.71	0.24	0.99	0.32
	85	0.09	0.036	0.075	0.74	0.54	1.89	1.7	0.04				
	(600)	(0.72)	(0.057)	(0.080)	(−28.51)	(−27.65)	(5.31)	(10.9)	(−26.04)		(0.75)		
	88	0.11	0.039	0.055	0.66	0.46	1.83	1.3	0.05				
IV	531	0.72	0.042	0.114	−29.20	−28.33	5.42	12.3	−25.59	1.14	0.27	0.99	0.38
	85	0.11	0.036	0.069	0.78	0.56	1.91	1.7	0.04				
	(616)	(0.71)	(0.061)	(0.095)	(−28.43)	(−27.56)	(5.59)	(10.9)	(−25.61)		(0.72)		
	104	0.10	0.046	0.074	0.86	0.64	1.54	1.8	0.04				
V	546	0.73	0.056	0.109	−29.10	−28.20	5.06	12.2	−24.98	1.74	0.20	0.91	0.28
	54	0.13	0.040	0.062	0.70	0.47	1.47	1.9	0.03				
	(663)	(0.71)	(0.073)	(0.093)	(−28.20)	(−27.32)	(5.20)	(10.2)	(−25.00)		(0.71)		
	145	0.12	0.053	0.057	0.95	0.72	1.75	1.9	0.04				

(c)

Case	T_{vib}	E_{vib}	E_{rot}	E_{tr}	E_p	E_f	r_I	N_f	E^0	E_R	$P_{C(R)}$	P_C+P_R	P_C/P_R
I	581	0.62	0.057	0.084	−28.43	−27.67	5.50	10.0	−26.01	0.	0.27	0.99	0.38
	92	0.10	0.040	0.058	(0.55)	0.35	1.59	1.0	0.06				
	(622)	(0.68)	(0.055)	(0.066)	−28.22	(−27.42)	(5.66)	(10.1)	(−26.02)		(0.72)		
	82	0.11	0.045	0.051	(0.50)	0.29	1.64	0.9	0.07				
II	553	0.66	0.049	0.089	−28.72	−27.92	5.81	10.9	−25.61	0.41	0.20	0.98	0.26
	63	0.10	0.045	0.046	0.46	0.27	1.71	1.0	0.07				
	(631)	(0.67)	(0.065)	(0.073)	(−28.13)	(−27.32)	(5.61)	(10.0)	(−25.61)		(0.78)		
	104	0.11	0.045	0.054	0.66	0.45	1.62	1.2	0.08				
III	593	0.68	0.073	0.093	−28.62	−27.77	5.17	10.7	−24.97	1.08	0.20	0.91	0.28
	101	0.09	0.044	0.056	0.67	0.48	1.81	1.6	0.08				
	(685)	(0.67)	(0.058)	(0.090)	(−27.92)	(−27.10)	(5.50)	(9.6)	(−24.97)		(0.71)		
	139	0.12	0.043	0.074	0.76	0.52	1.65	1.4	0.07				
IV	619	0.73	0.047	0.158	−28.61	−27.67	4.98	10.6	−24.06	1.90	0.08	0.85	0.10
	85	0.07	0.036	0.125	0.67	0.44	1.37	1.3	0.04				
	(777)	(0.73)	(0.093)	(0.116)	(−27.79)	(−26.85)	(5.18)	(9.4)	(−24.12)		(0.77)		
	256	0.16	0.079	0.072	1.11	0.80	1.78	1.5	0.07				

TABLE II. Averaged results for the reaction $[Na_4Cl_3]^+Ar_{12}+Cl^-$, for constant value of the total energy of the system $E^0=-25.6$ eV. All quantities are as defined in the caption to Table I. T^0_{vib} is the average initial temperature of the target cluster. For each case (corresponding to different partitioning of the total energy, and thus to different values of E_R and T^0_{vib}) the mean values in the first row are for cube-isomer products and those in parenthesis are for ring-isomer products. For both product forms the values in the row under the mean values are the standard deviations from the mean.

Case	T_{vib}	E_{vib}	E_{rot}	E_{tr}	E_p	E_f	r_I	N_f	T^0_{vib}	E^0	E_R	$P_{C(R)}$	P_C+P_R	P_C/P_R
I	502	0.69	0.051	0.099	−29.30	−28.46	4.39	12.6	31.6	−25.61	1.90	0.27	0.82	0.49
	82	0.12	0.037	0.058	0.75	0.54	1.80	1.8		0.01				
	(606)	(0.72)	(0.060)	(0.100)	(−28.55)	(−27.67)	(5.68)	(11.0)	(31.6)	−25.60		(0.55)		
	120	0.10	0.040	0.060	0.90	0.68	1.53	1.9		0.01				
II	531	0.72	0.042	0.114	−29.20	−28.33	5.42	12.3	189	−25.59	1.14	0.27	0.99	0.38
	85	0.11	0.036	0.069	0.78	0.56	1.91	1.7		0.04				
	(616)	(0.71)	(0.061)	(0.095)	(−28.43)	(−27.56)	(5.59)	(10.9)	(189)	(−25.61)		(0.72)		
	104	0.10	0.046	0.074	0.86	0.64	1.54	1.8		0.04				
II	553	0.66	0.049	0.089	−28.72	−27.92	5.81	10.9	316	−25.61	0.41	0.20	0.98	0.26
	63	0.10	0.045	0.046	0.46	0.27	1.71	1.0		0.07				
	(631)	(0.67)	(0.065)	(0.073)	(−28.13)	(−27.32)	(5.61)	(10.0)	(316)	(−25.61)		(0.78)		
	104	0.11	0.045	0.054	0.66	0.45	1.62	1.2		0.08				

fixed initial (vibrational) temperature [31.6, 189, and 316 K in Tables I(a), I(b), and I(c), respectively] of the equilibrated $[Na_4Cl_3]^+Ar_{12}$ reactant, with variable E_R ranging from 0.0 to 4.517 eV, and (ii) fixed total energy of the reaction system, $E^0 = -25.605$ eV, (in Table II) distributed between E_R and the energy of the initial cluster (E_c^0);

$$E^0 = E_R + E_c^0, \tag{2a}$$

$$E_c^0 = E_{kc}^0 + E_{pc}^0, \tag{2b}$$

$$E_{kc}^0 = E_{\text{rot}}^0 + E_{\text{vib}}^0, \tag{2c}$$

where E_{kc}^0 and E_{pc}^0 are the initial kinetic and potential energies of the cluster, respectively, and E_{rot}^0 and E_{vib}^0 correspond to the initial rotational and vibrational energies. [The initial vibrational temperature of the cluster is determined from $k_B T_{\text{vib}}^0 = 2E_{\text{vib}}^0/3(N-2)$, where N is the total number of atoms in the initial reactant cluster.]

In all cases which we have investigated, the large majority of reactions result in neutral $[Na_4Cl_4]Ar_q$ mixed clusters, with the alkali-halide component in either the cube or ring isomeric forms. In our discussion of reactions with fixed initial temperature of the reactant cluster, we focus on the case with $T_{\text{vib}}^0 = 31.6$ K. Similar trends are found for the other initial temperatures (see also our discussion in Sec. III). A typical distribution of the potential energies, E_p', of the alkali-halide component in the product mixed clusters, is shown in Fig. 4 for the reaction conditions $T_{\text{vib}}^0 \simeq 31.6$ K, $E_R = 1.08$ eV [see Table I(a), case III]. The energetic distinction between the two isomers is evident from the figure. Distributions, for the two isomers, of the product mixed clusters' total energy (E_f) and of the translational (E_{tr}), rotational (E_{rot}), and vibrational (E_{vib}) energies, as well as of the products' vibrational temperatures T_{vib}, are given in Fig. 5. As seen from the figure, of all the degrees of freedom, the energy associated with vibrational motion is the largest. In addition, we observe that T_{vib} for the lower-potential-energy isomer (cube) is somewhat lower than the one corresponding to the next higher-in-energy isomer (ring).

From inspection of Tables I(a)–I(c) (constant initial vibrational temperatures $T_{\text{vib}}^0 = 31.6$, 189, and 316 K, respectively) the following systematic trends can be deduced:

(i) The probability for reaction $P_C + P_R$, where P_C and P_R are the probabilities for occurrence in the product of the cube and ring isomeric forms of Na_4Cl_4, respectively, is high

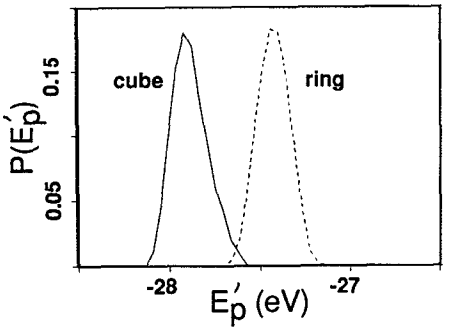

FIG. 4. Interionic potential energy distributions, $P(E_p')$, for cube and ring products of the reaction $[Na_4Cl_3]^+Ar_{12} + Cl^-$ for case III in Table I(a). The distributions were separately normalized to unity for each isomer.

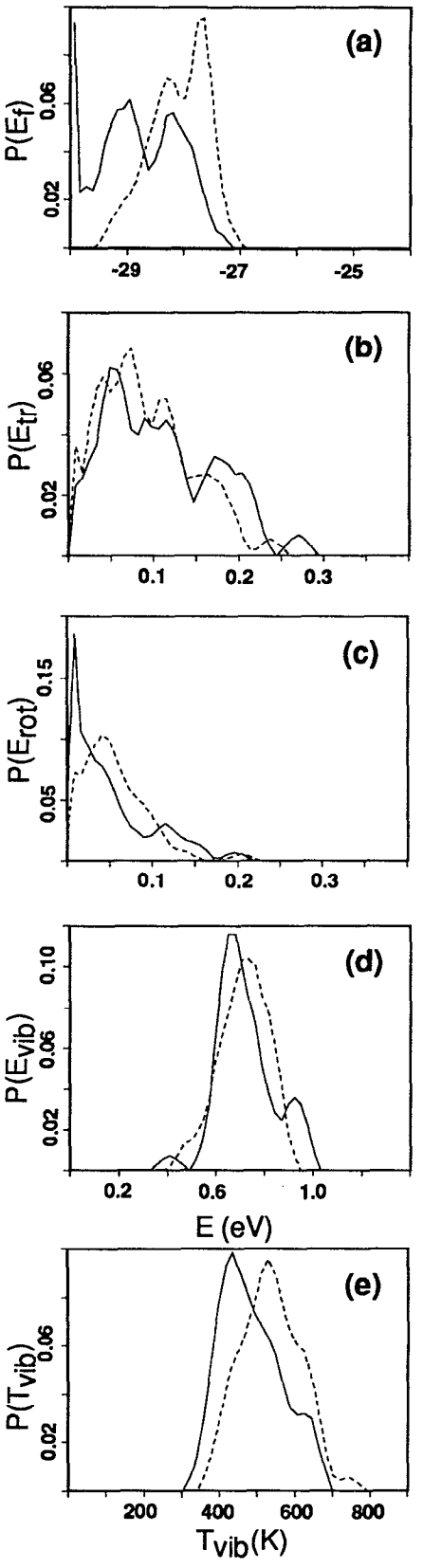

FIG. 5. Distributions of the total (E_f), translational (E_{tr}), rotational (E_{rot}), vibrational (E_{vib}) energies, and of the vibrational temperature (T_{vib}) of the products of the reaction corresponding to case III in Table I(a). Solid and dashed lines correspond to cube and ring isomers of the Na_4Cl_4 embedded product clusters. The distributions were separately normalized to unity for the two isomers. Energies in eV and temperature in K.

for small relative translational energies between the reactants, and decreases upon increasing E_R.

(ii) The branching ratio P_C/P_R, exhibits a decreasing trend upon increasing E_R, i.e., the probability for a final product with the alkali-halide component in the lower-energy isomeric form (cube) increases upon decreasing the relative impact translational energy between the reactants (see also discussion in Sec. IV, and Fig. 16 there). We also observe that for a given value of E_R, P_C/P_R decreases for initially vibrationally hotter reactant clusters.

(iii) The reaction between $[Na_4Cl_3]^+Ar_{12}$ and Cl^- results in loss of argon atoms in the final product $[Na_4Cl_4]Ar_{q'}$ clusters, with q' insensitive to E_R for the cube isomers [e.g., $q' \sim 5$ i.e., loss of ~ 7 argon atoms with reference to the initial cluster for $T^0_{vib} = 31.6$ K, see Table I(a) where the number of atoms in the product cluster, N_f, is given; $q' = N_f - 8$]. For the ring-isomer products q' is smaller than for the cube-isomer clusters, exhibiting a decreasing trend with increasing E_R (i.e., more argon atoms are lost from the initial cluster). In almost all cases we have observed that the released argons appear in the form of monomers. We also note that the number of Ar atoms remaining attached to the product alkali-halide cluster is smaller when the vibrational temperature (T^0_{vib}) of the initial reactant charged cluster is higher due to the higher energy content of these systems (compare N_f values in Tables I(a)–I(c)].

(iv) The vibrational temperatures of the cube-isomer products remain about constant for all E_R, and their distributions peak at lower values than those corresponding to the ring-isomer products. The latter exhibit an increasing trend with increasing E_R. In all cases, the vibrational energy is equally partitioned between the alkali-halide and remaining argon atoms in the product mixed clusters, i.e., the products are at internal equilibrium.

(v) For low E_R, the mean values of the impact parameter distributions, corresponding to the two final products (mixed-clusters with cube or ring-alkali-halide isomers), are close to that of a random distribution ($\bar{r}_{imp} \simeq 5.3$ Å) and exhibit a tendency to decrease upon increasing E_R.

Unlike the results given in Tables I(a)–I(c), which were obtained from simulations at *constant initial vibrational temperatures*, T^0_{vib}, those shown in Table II were obtained for *constant initial energy* E^0 of the reaction system [cases IV in Tables I(a) and I(b) and case II in Table I(c)], partitioned in three different ways between the initial relative translational energy (E_R) and initial internal energy (E^0_c) of the target cluster (corresponding to the three different initial vibrational temperatures T^0_{vib}). As seen, while the probability for cube-isomer products (P_C) is roughly constant for the three cases, the probability for producing ring-isomers increases upon increasing the initial cluster vibrational temperature, T^0_{vib}, (and correspondingly decreasing, E_R), resulting in a net decreasing trend in the branching ratio P_C/P_R. Additionally, we note that as in the constant T^0_{vib} case, the cube-isomer products are colder than the higher-isomer ones, and that more argon atoms are released for the latter.

From these results and those given in Tables I(a)–I(c), we deduce that while for reactions at constant initial T^0_{vib} the product branching ratio (P_C/P_R) exhibits a downward trend with increasing initial relative translation energy between the reactants, T^0_{vib} is the controlling parameter for reactions at constant initial total energy.

To investigate the dependence of the product distribution on the size of the initial target cluster we show in Table III results for the reaction $[Na_4Cl_3]^+Ar_{32} + Cl^-$, at $T^0_{vib} = 31.6$ K and $E_R = 2.14$ eV. First we note that the overall probability for reaction ($P_C + P_R$), as well as the branching ratio (P_C/P_R), are somewhat higher now than those corresponding to the closest case for the smaller system [see Table I(a), case IV], although E_R is slightly higher here. Furthermore, we observe that the vibrational temperatures of the cube- and ring-isomeric products are essentially equal and significantly lower than the final (unequal) temperatures of the products obtained via the corresponding reaction of the smaller cluster. The number of Ar atoms released in the course of reaction is ~ 17 (mostly all as monomers). These results indicate that embedding the reactants in larger argon clusters leads to improved annealing efficiency, resulting in colder products and enhanced probability for generation of ground state (lowest-in-energy) isomers.

2. Reaction dynamics

The dynamics of the reactions discussed in the previous subsection can be explored using the results displayed in Figs. 6–10. As before, for the smaller system we show results for $T^0_{vib} = 31.6$ K. Similar conclusions are obtained for the two higher initial temperatures.

In Fig. 6 we show, vs time (in ps), the number of Ar atoms released in the reaction $[Na_4Cl_3]^+Ar_{12} + Cl^-$ and their kinetic energy for the reaction systems I, IV, and V in Table I(a). (Here and elsewhere an Ar atom is identified as a released atom when its distance from any other atom in the system is larger than 7.9 Å.) In these figures we plot sepa-

TABLE III. Averaged results for the reaction $[Na_4Cl_3]^+Ar_{32} + Cl^-$ at $T^0_{vib} = 31.6$ K and $E_R = 2.14$ eV. All quantities are as defined in the caption to Table I.

Case	T_{vib}	E_{vib}	E_{rot}	E_{tr}	E_p	E_f	r_I	N_f	E^0	E_R	$P_{C(R)}$	$P_C + P_R$	P_C/P_R
I	322	0.88	0.027	0.061	−32.53	−31.56	5.50	23.1	−28.88	2.14	0.34	0.90	0.61
	54	0.09	0.020	0.037	0.83	0.68	1.79	3.2	0.07				
	(335)	(0.95)	(0.033)	(0.051)	(−32.33)	(−31.29)	(5.24)	(23.4)	(−28.88)	(2.14)	(0.56)		
	47	0.13	0.020	0.038	0.84	0.65	1.67	3.1	0.07				

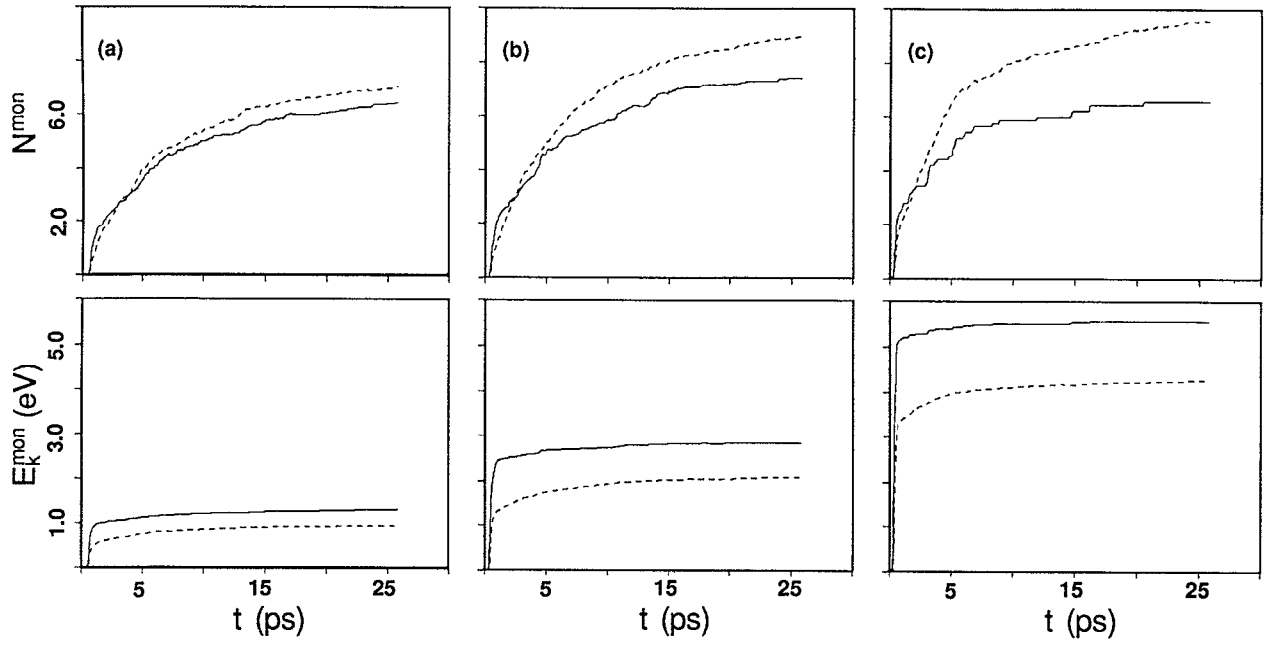

FIG. 6. Number of released Ar monomers (N^{mon}) and their cumulative kinetic energy (E_k^{mon}) vs time for the reaction systems I, IV, and V in Table I(a), shown in (a)–(c), respectively. Solid and dashed lines correspond to cube- and ring-isomer products, respectively. Note that the major part of the energy is carried by the first one or two released Ar atoms. Also note that for reactions yielding ring isomers, the number of released Ar atoms is larger than for those resulting in cube isomers. However, the energy carried by the released atoms in reactions yielding the cube isomer is larger.

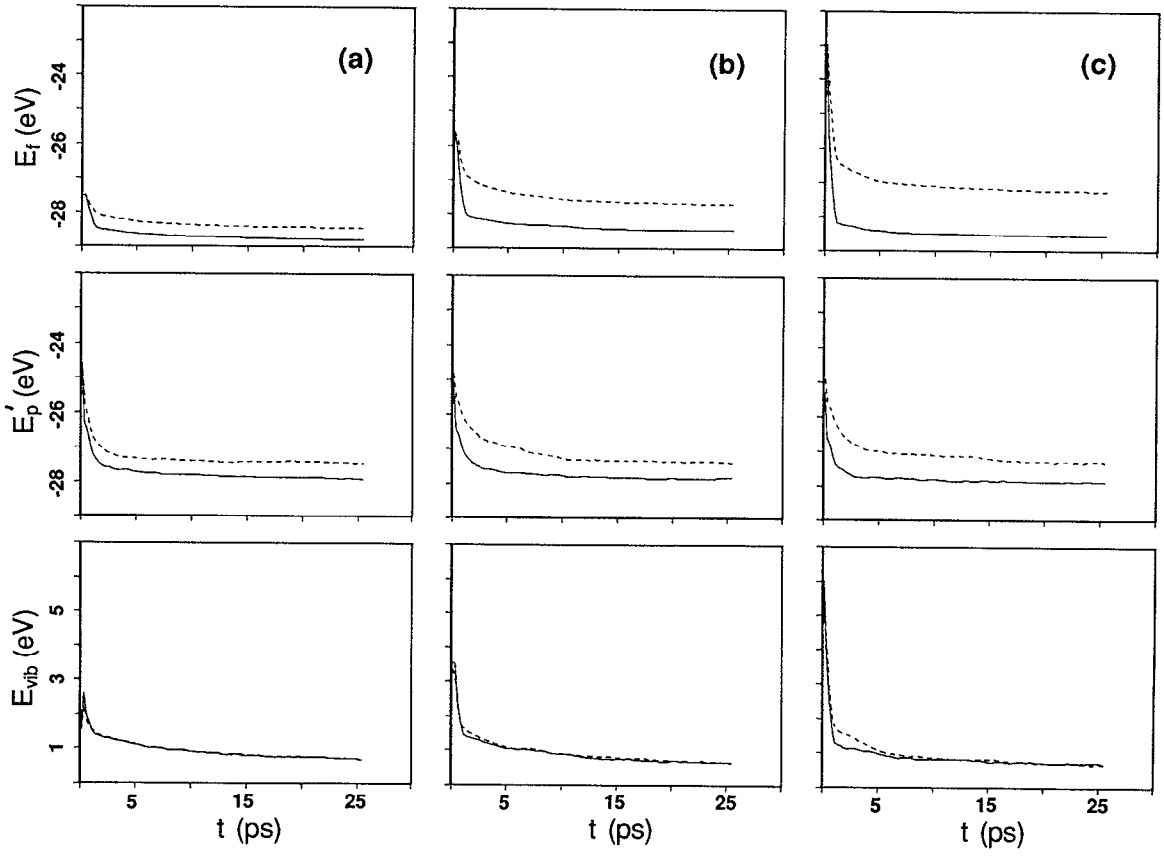

FIG. 7. Total (E_f), interionic potential (E_p') and vibrational (E_{vib}) energies vs time for the reaction systems I, IV, and V in Table I(a), shown in (a)–(c), respectively. Solid and dashed lines correspond to cube- and ring-isomer products. Note the fast formation of the structural isomeric forms and the lack of interconversion between them.

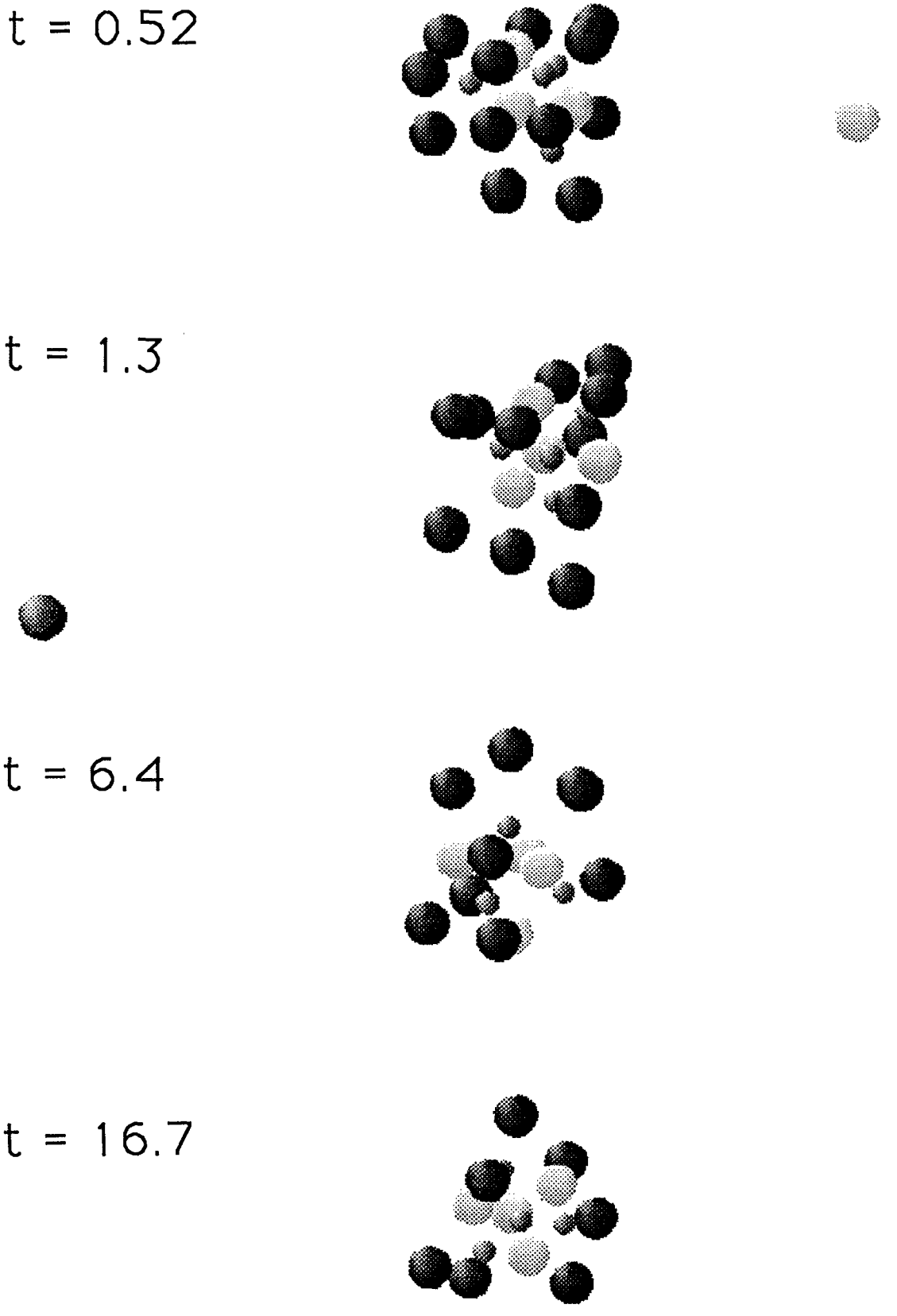

FIG. 8. Selected configurations for the reaction $[Na_4Cl_3]^+Ar_{12} + Cl^-$ [case IV in Table I(a)] at $t = 0.52$, 1.3, 6.4, and 16.7 ps, resulting in $[Na_4Cl_4]Ar_7$ with the alkali-halide in the groundstate, cube-isomer structure. Dark spheres represent Ar atoms. Large light and small grey spheres represent Cl^- and Na^+ ions. Note that the impulsive collision with the Cl^- ion leads to ejection of a highly energetic Ar atom at an early time. The times are with respect to the collision partners separated at $t = 0$ by 31.8 Å.

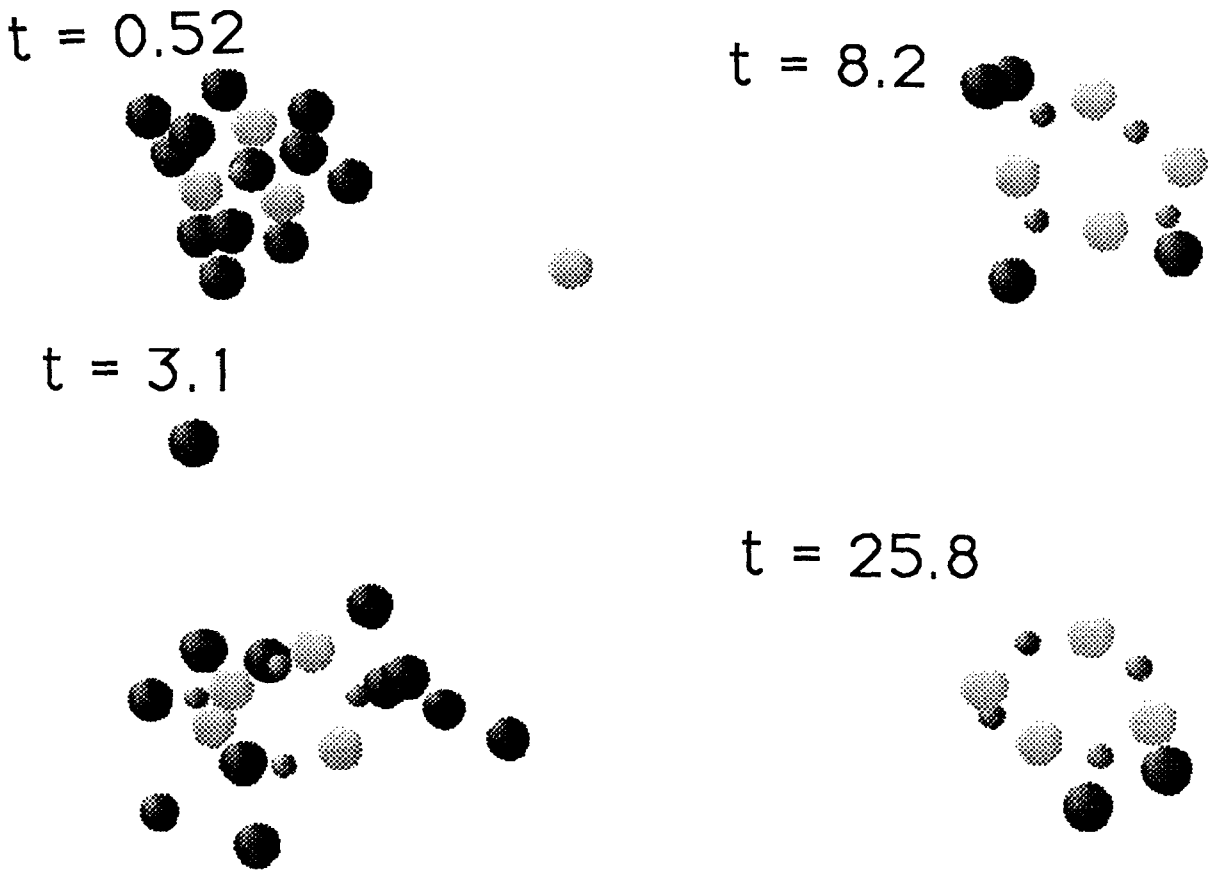

FIG. 9. Selected configurations for the reaction $[Na_4Cl_3]^+Ar_{12} + Cl^-$ [case IV in Table I(a)] at $t = 0.52$, 3.1, 8.2, and 25.8 ps, resulting in $[Na_4Cl_4]Ar_2$ with the alkali-halide in the ring-isomeric structure. See also caption to Fig. 8. Note that the collision with the Cl^- ions results in an ejection of an Ar atom at a later time than that shown in Fig. 8, and that after the collision the structure of the cluster is less compact indicating a redistribution of the imparted energy, resulting in gradual evaporation of Ar atoms at later times.

rately results which lead to the formation of cube (solid line) and ring (dashed line) isomers.

As evident from Fig. 6, the initial collision of the Cl^- reactant with the cluster leads to an impulsive ejection of one or two Ar atoms which carry a large fraction of the total energy released overall in the reaction. Moreover, events in which the Cl^- loses more energy in the first collision (i.e., ejecting a faster Ar atom) are more likely to result in the ground state (cube) isomer. The Ar atoms which are subsequently released are much slower, and the size of the product clusters decrease exponentially, with more Ar atoms released in the course of reactions leading to the higher-in-energy alkali-halide isomer [see in particular Fig. 6(c)].

Inspection of the time evolutions of the total and vibrational energies of the product cluster (E_f and E_{vib}) and of the interionic potential energy (E_p'), given in Fig. 7, shows that the product species (cube or ring isomers) are formed in the very initial stage of the collision, and that no interconversion occurs between the two isomeric forms. Subsequent to formation in the initial stage, further structural annealing accompanied by cooling (see E_{vib}) occurs via release of Ar atoms. Selected atomic configurations during reactions lead-

TABLE IV. Averaged results for the reaction between Cl^- with $[Na_{14}Cl_{12}]^{+2}Ar_{30}$ (case I), and with $[Na_{14}Cl_{12}]^{+2}$ (case II). P_C and P_D are the probabilities for formation of cubic and disordered isomers, respectively. All other quantities are as defined in the caption to Table I. Results for the disordered isomers in parenthesis.

Case	T_{vib}	E_{vib}	E_{rot}	E_{tr}	E_p	E_f	r_I	N_f	E^0	E_R	$P_{C(D)}$	$P_C + P_D$	P_C/P_D
I	407	2.71	0.039	0.041	−110.0	−107.2	6.08	53.0	−104.72	3.06	0.54	0.97	1.26
	51	0.31	0.030	0.026	1.5	1.1	1.92	1.4	0.02				
	(452)	(2.97)	(0.065)	(0.029)	(−109.2)	(−106.1)	(6.51)	(52.7)	(−104.72)	(3.06)	(0.43)		
	44	0.27	0.041	0.024	1.4	1.0	1.76	1.5	0.02				
II	(868)	(2.81)	(0.19)	(0.0)	(−94.5)	(−91.49)	(6.19)	(27)	(−91.49)	(1.45)	(0.84)		
	25	0.08	0.10		0.2	0.02	2.14		0.02				

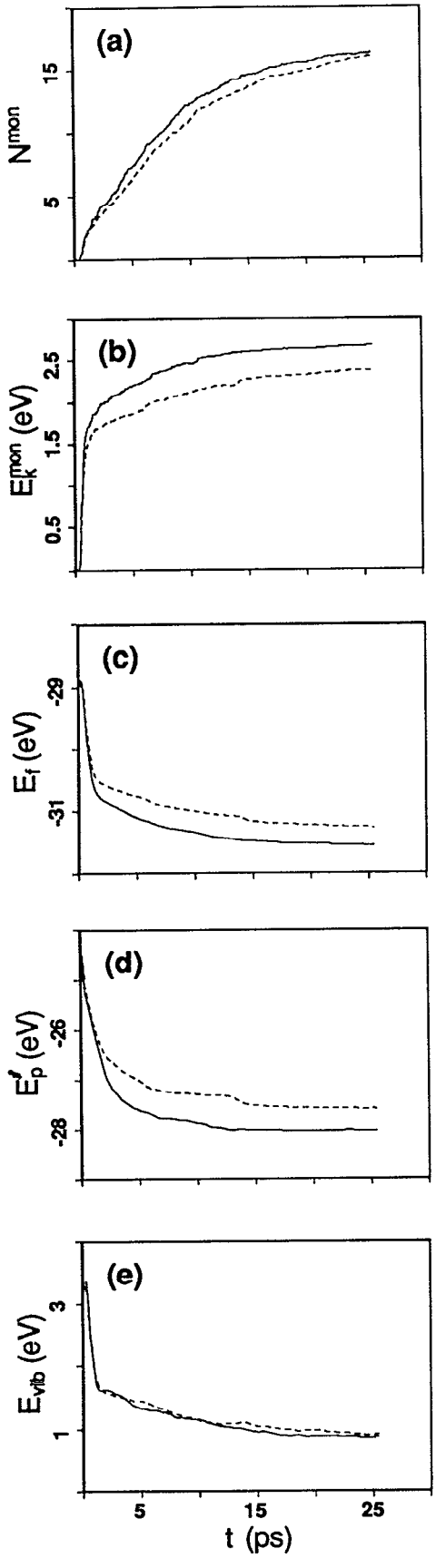

FIG. 10. Averaged number of ejected Ar monomers (N^{mon}), and their cumulative kinetic energy (E_k^{mon}), and the total (E_f), interionic potential (E'_p), and vibrational (E_{vib}) energies, plotted vs time for the reaction $[Na_4Cl_3]^+Ar_{32} + Cl^-$. Solid and dashed lines correspond to cube- and ring-isomer products, respectively. Energy in eV and time in ps.

ing to the formation of cube and ring isomers are shown in Figs. 8 and 9, respectively. (Descriptions of the trajectories are given in the figure captions).

Results pertaining to the dynamics of the reaction $[Na_4Cl_3]^+Ar_{32} + Cl^-$ are shown in Fig. 10, exhibiting similar trends to those discussed above, although the fraction of the energy released in the reaction, beyond that carried by the Ar atom ejected during the first collision with the Cl^-, is larger in this case [compare Fig. 10(b) with the E_k^{mon} curves in Fig. 6]. Furthermore, we observe [e.g., compare the rate of decrease of E'_p in Figs. 10(d) and the corresponding one for the smaller system in Fig. 7(b)] that because of the larger embedding environment (i.e., second shell of Ar atoms) the process of alkali-halide isomer formation is slower in the larger system.

B. $[Na_{14}Cl_{12}]^{+2}Ar_{30} + Cl^-$

Prior to discussing results obtained in simulations of the reaction between a Cl^- anion and a $[Na_{14}Cl_{12}]^{+2}Ar_{30}$ cluster, whose initial vibrational temperature is 31.6 K, we remark on the reaction between Cl^- and a bare $[Na_{14}Cl_{12}]^{+2}$ cluster with the same initial temperature. Results for the latter system (averaged over 100 collisions) are given in Table IV (Case II). The main product (84%) of this reaction is a highly disordered $[Na_{14}Cl_{13}]^+$ cluster. Other products of this reaction (16%) include fragmentation, typically into $NaCl + [Na_{13}Cl_{12}]^+$.

Averaged results for the reaction $[Na_{14}Cl_{12}]^{+2}Ar_{30} + Cl^-$ are given in Table IV (case I), and in Figs. 11 and 12. The total probability for forming a $[Na_{14}Cl_{13}]^+Ar_{q'}$ product in this reaction is high. The alka-

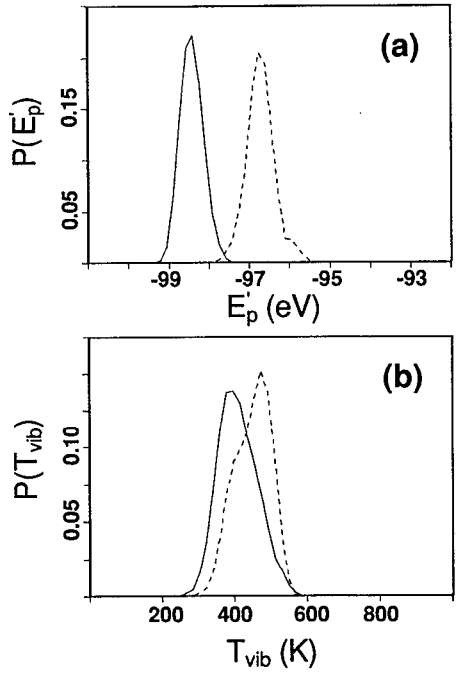

FIG. 11. Interionic potential energy [in (a)] and cluster vibrational temperature [in (b)] for the reaction $[Na_{14}Cl_{12}]^{+2}Ar_{30} + Cl^-$ (case I in Table IV). Solid and dashed lines correspond to cubic and disordered isomers of the $[Na_{14}Cl_{13}]^+$ component in the products. Energy in eV and temperature in K.

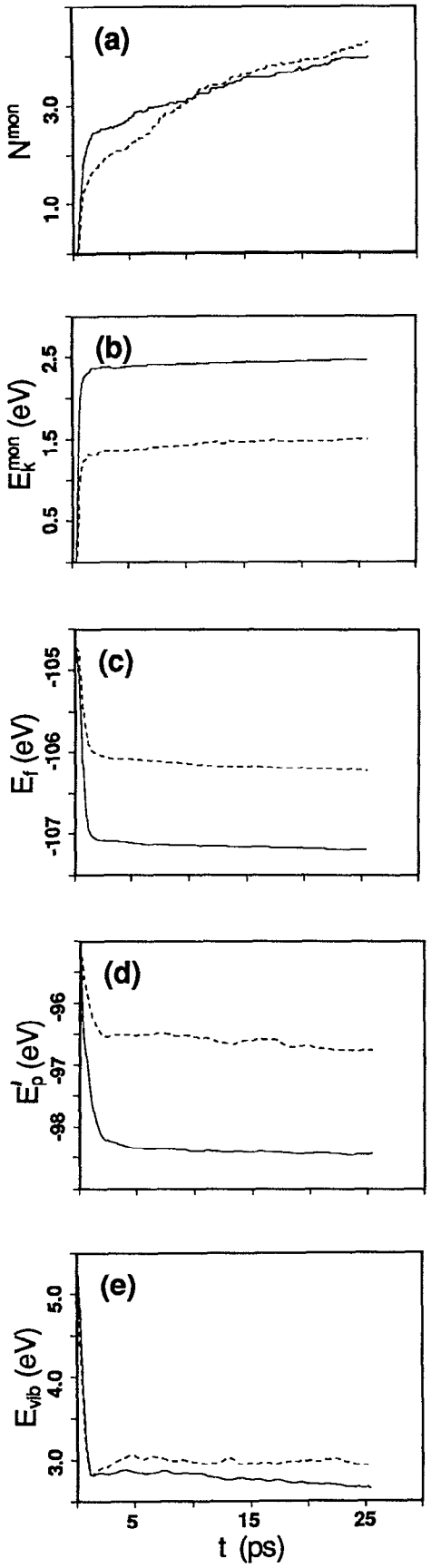

FIG. 12. Same as Fig. 10, for the reaction $[Na_{14}Cl_{12}]^{+2}Ar_{30} + Cl^-$. Solid and dashed lines correspond to cubic and disordered isomers of the $[Na_{14}Cl_{13}]^+$ component in the products. Energy in eV and time in ps.

li-halide component in the product clusters form either an ordered $3\times3\times3$ cubic structure or a number of nearly degenerate higher-in-energy isomers of less ordered nature, typically incorporating Ar atoms inside the structure (the corresponding probabilities for the ordered (cubic) and disordered products are denoted as P_C and P_D, respectively). The energetic distinction between the cubic and disordered isomers is evident from Fig. 11(a) where we show the distribution of interionic potential energies of the reaction products. Note, in addition, that the potential energies of these products are significantly lower (more negative) than that for the reaction of the bare $[Na_{14}Cl_{12}]^{+2}$ cluster (see Table IV, case II, column E_p). The cubic-isomer products are characteristically colder than the disordered ones [see Fig. 11(b)], and both are much colder vibrationally than the products of the bare cluster reactions (see Table IV).

The dynamics of the reaction displayed in Fig. 12, exhibits similar characteristics to that of the reactions of the smaller clusters described in Sec. III A. The major part of the energy release occurs in the very initial stage of the collision, resulting in the ejection of one or two Ar monomers [see Figs. 12(a) and 12(b)]. The tendency toward statistical redistribution of energy in this relatively large system is reflected in the small number of Ar atoms which are released past the initial impact (on the average a total of four monomers). In accord with our previous observation, the amount of energy carried by the ejected Ar atoms in the initial collision stage determines the reaction path, i.e., a larger energy loss is more likely to result in a cubic-isomer structure.

Configurations, at selected times, for reactions resulting in a cubic and disordered isomers are shown in Figs. 13 and 14, respectively. (Descriptions of the reaction trajectories are given in the captions.)

C. Other collision events

In addition to the reactions discussed in the previous subsections, other reaction and collision events occur. For the reaction system $[Na_4Cl_3]^+Ar_{12} + Cl^-$ with the initial vibrational temperature of the cluster $T^0_{vib} = 31.6$ K, the onset for these events is for a relative translational energy between the reactants $E_R \simeq 1$ eV, for the range of impact parameters which we sampled. For initially hotter clusters the onset of such events occurs at somewhat lower values of E_R.

Results for such events for the conditions of case IV in Table I(a) are given at the bottom of the table. We observe that in both cases the average vibrational temperature of the large component of the products (i.e., $[Na_3Cl_3]Ar_{q'}$ in the case of a dimer forming reaction, and $[Na_4Cl_3]^+Ar_{q'}$ for a glancing reaction) is significantly colder than in the case of the corresponding association reactions (see case IV). This effect, which is particularly noted for the glancing collisions, is characteristic to a spectator mechanism of the collisions which lead to stripping (i.e., dimer formation) or glancing. In these collision events the interaction between the Cl^- and the cluster is relatively localized, with the major part of the target cluster playing the role of a spectator. Furthermore, we note that these collision events are characterized by larg-

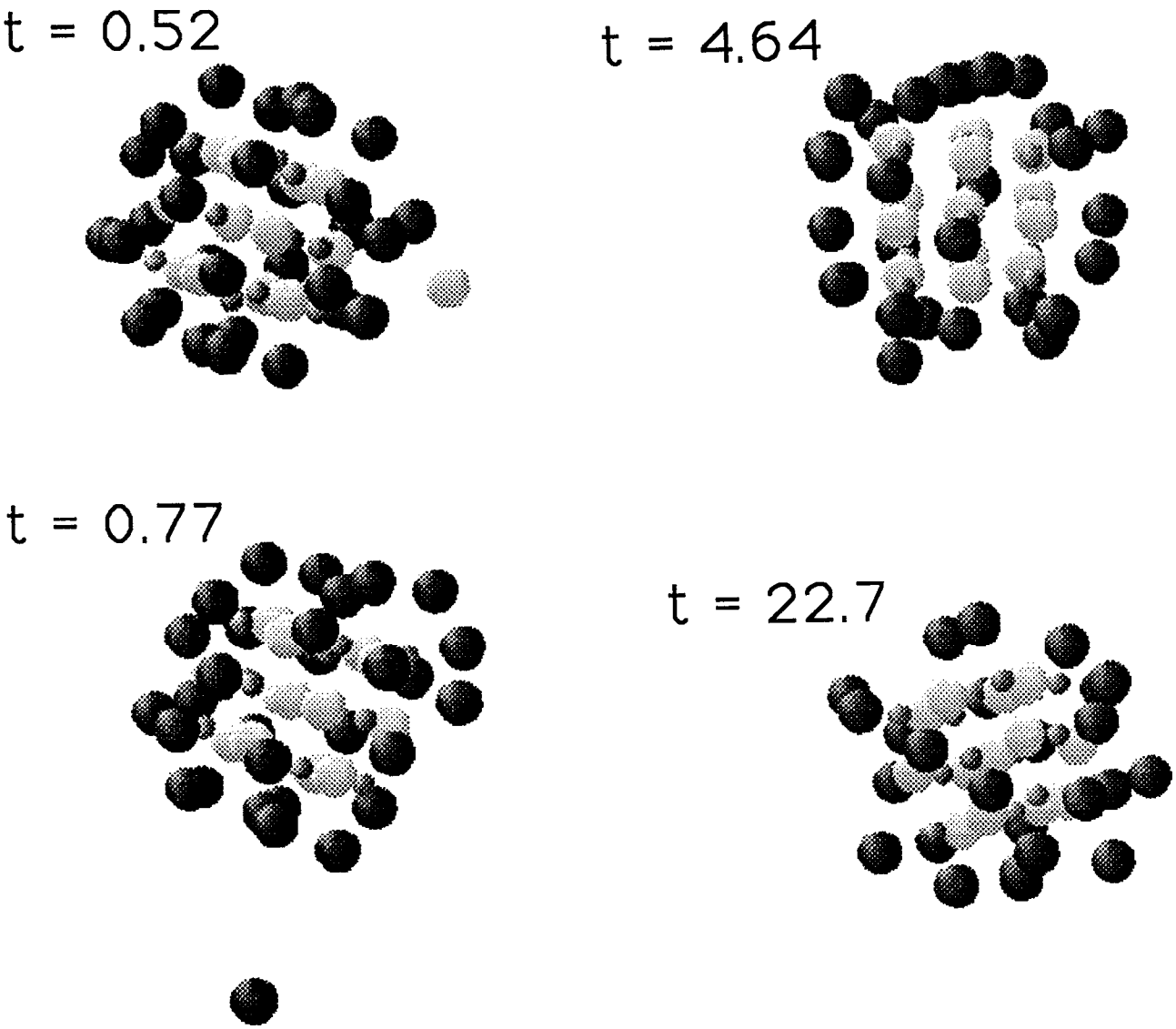

FIG. 13. Selected configurations for the reaction $[Na_{14}Cl_{12}]^{+2}Ar_{30} + Cl$, at $t = 0.52$, 0.77, 4.64, and 22.7 ps, resulting in $[Na_{14}Cl_{13}]^{+}Ar_{25}$ with the alkali-halide in the cubic isomer structure. Note that the incoming Cl initially ejects a fast Ar atom and attaches without much distortion of the original reactant structure.

er average impact parameters than in those corresponding to the association reactions [compare r_I's in Table I(a)]. A typical set of configurations along the trajectory of a reaction leading to the formation of a NaCl molecule and $[Na_3Cl_3]Ar_{q'}$ is shown in Fig. 15. A similar set of nonassociative collision events, exhibiting the characteristics of a spectator mechanism,[15] is observed for the other reaction systems which we have investigated.

IV. SUMMARY

In this study we have proposed and investigated a new class of cluster-catalyzed reactions (CCR). This mode of cluster reactions focuses on the role of the cluster environment as a local heat bath. To demonstrate the concept we have performed extensive classical molecular dynamics simulations for charged alkali-halide fragments, embedded in various sizes of argon clusters colliding with an incident Cl^-, for various collision conditions.

Two reaction systems have been investigated: (i) $[Na_4Cl_3]^+Ar_q + Cl^-$ ($q = 12$ and 32); and (ii) $[Na_{14}Cl_{12}]^{+2}Ar_{30} + Cl^-$. In both cases we focus on the association reactions leading to the production of $[Na_4Cl_4]Ar_{q'}$ ($q' \leqslant q$) for (i), where the alkali-halide component may be in either its lowest energy cubic isomeric form or in a higher-energy structural isomer (ring structure), and for the larger cluster (ii), the alkali-halide in the product cluster $[Na_{14}Cl_{13}]^+Ar_{q'}$ ($q' \leqslant 30$), may be found in either a cubic or disordered isomeric structures.

Our main results may be summarized as follows:

(a) Reactions between cold (and even more so for hot) bare $[Na_4Cl_3]^+$ clusters with Cl^- result in fragmentation or high-potential-energy isomers (chains); even for small relative translational energy between the reactants. Reac-

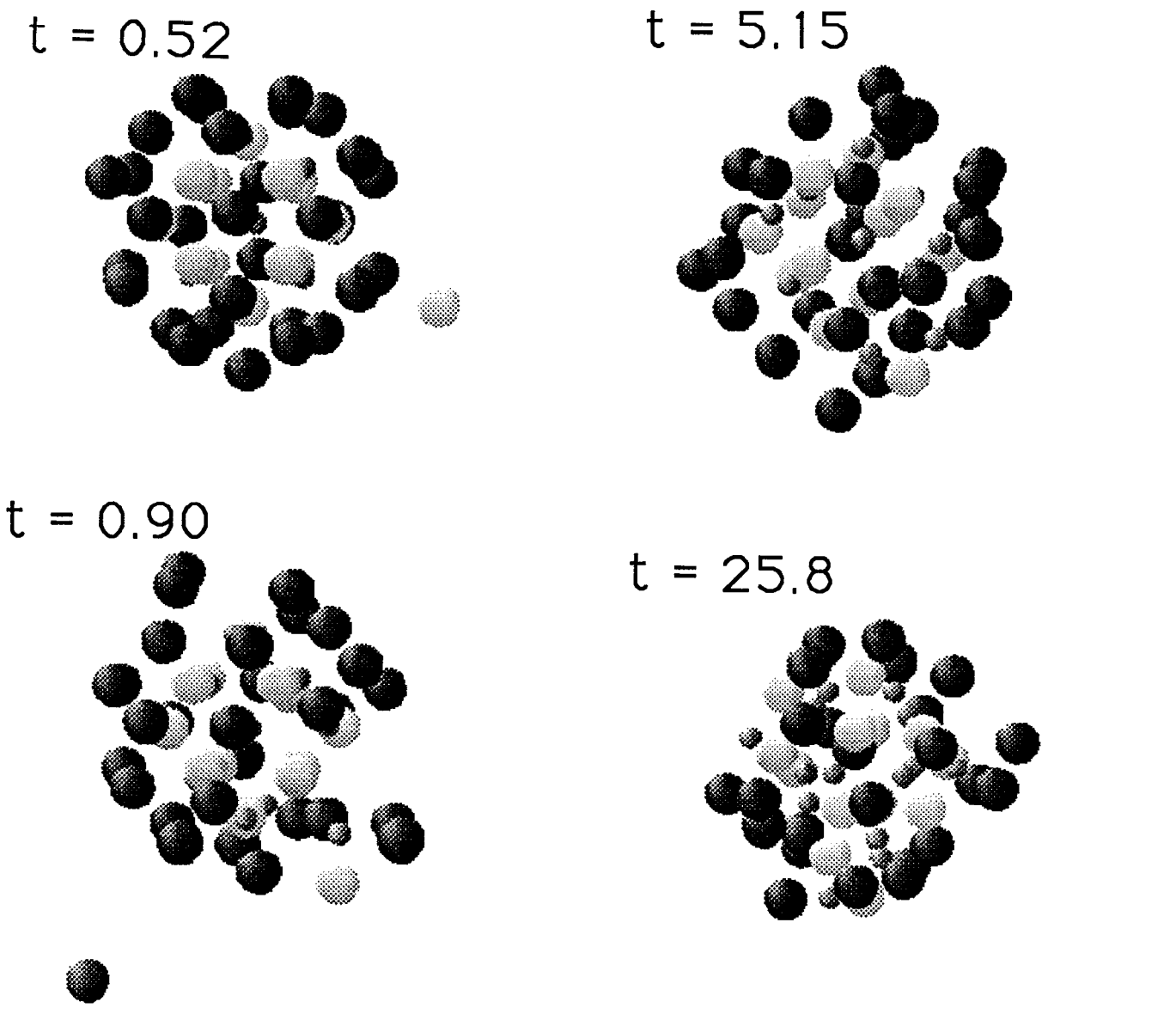

FIG. 14. Selected configurations for the reaction $[Na_{14}Cl_{12}]^{+2}Ar_{30} + Cl^-$, at $t = 0.52$, 0.90, 5.15, and 25.8 ps, resulting in $[Na_{14}Cl_{13}]^+Ar_{24}$, with the alkali-halide in a disordered isomeric structure. The initial collision with the target cluster causes the ejection of an Ar monomer and an appreciable distortion of the alkali-halide fragment. Further evolution involves the penetration (solvation) of Ar atoms into the alkali-halide structure, resulting in a relatively vibrationally hot disordered structure.

tions of Cl^- with bare $[Na_{14}Cl_{12}]^{+2}$ result in highly disordered $[Na_{14}Cl_{13}]^+$ isomers, or lead to fragmentation.

(b) For a *given initial vibrational temperature* of the reactant cluster, the total average probability for associative reaction products shows a decreasing trend with increasing relative translational energy (E_R) between the reactants. Other collision events which occur for high E_R are stripping reactions and glancing collisions. In both the later cases the products are vibrationally colder than for the corresponding associative reactions, illustrating a spectator mechanism.

(c) The averaged results for the branching ratios plotted vs E_R for the reaction $[Na_4Cl_3]^+Ar_{12} + Cl^-$, for three initial vibrational temperatures of the target clusters [$T^0_{vib} = 31.6$, 189, and 316 K, see Tables I(a)–I(c), respectively] are summarized in Fig. 16. These results show that for associative reactions with the reactant clusters at the same initial temperature, the branching ratio, P_C/P_R between the probability to produce the ground state isomer (cube) to that of producing the higher-energy isomer (ring), decreases with increasing E_R. Examination of the individual probabilities (P_C and P_R) for producing products with the alkali-halide in the cube and ring isomeric forms [see Tables I(a)–I(c)] indicates that the main trend correlating with the above conclusion is the systematic decrease in cube-isomer products (P_C) with increasing E_R.

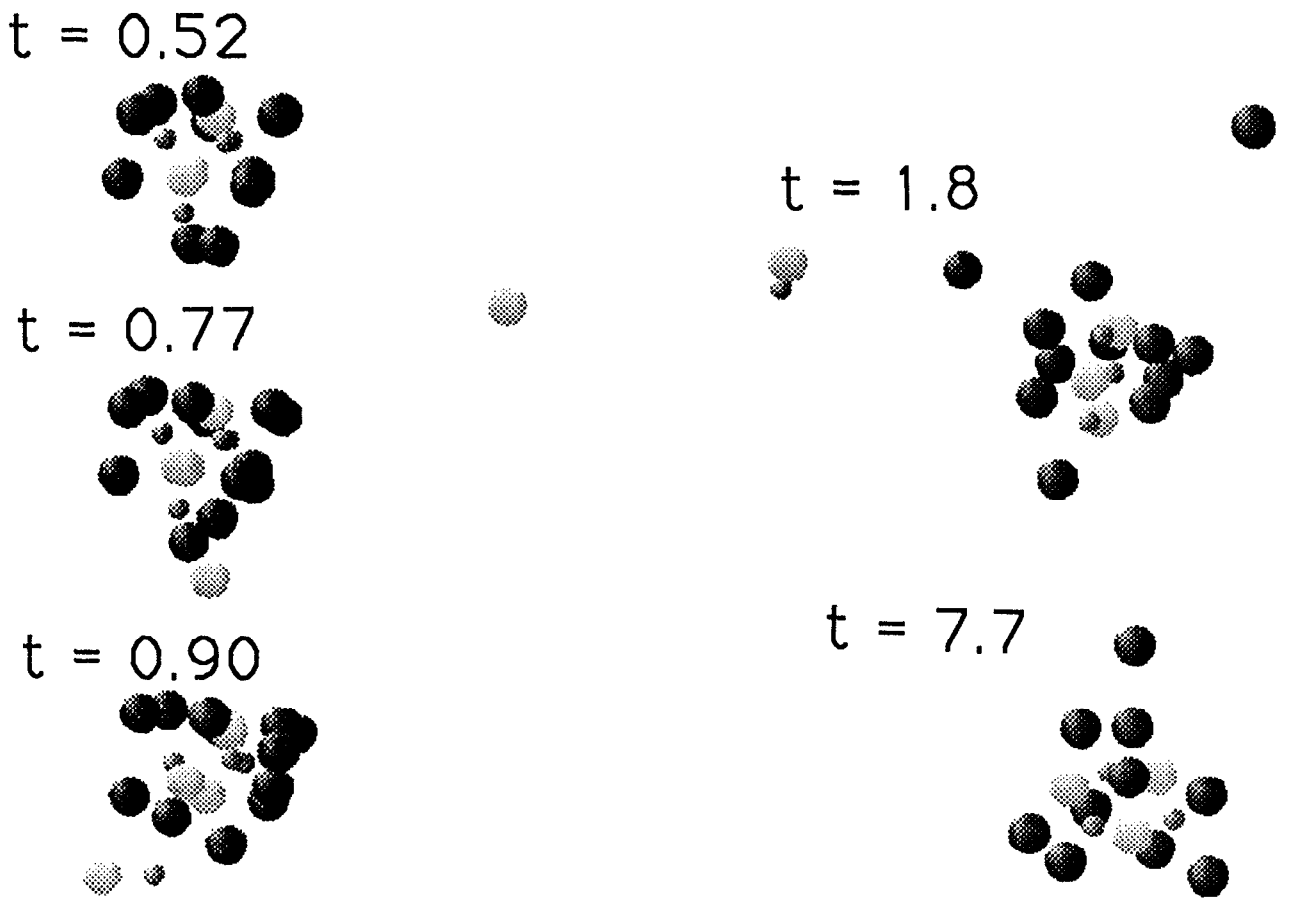

FIG. 15. Selected configurations for the stripping reaction $[Na_4Cl_3]^+Ar_{12} + Cl^- \rightarrow [Na_3Cl_3]Ar_{10} + NaCl$, at $t = 0.52$, 0.77, 0.90, 1.8, and 7.7 ps. Note the NaCl dimer at $t = 0.9$ ps and $t = 1.8$ ps.

(d) For a given size of the alkali-halide fragment, reactions in which the argon environment in the reactant cluster is larger [e.g., compare results for $q = 12$ and 32 for reaction system (i)] yield a higher proportion of ground state isomer products.

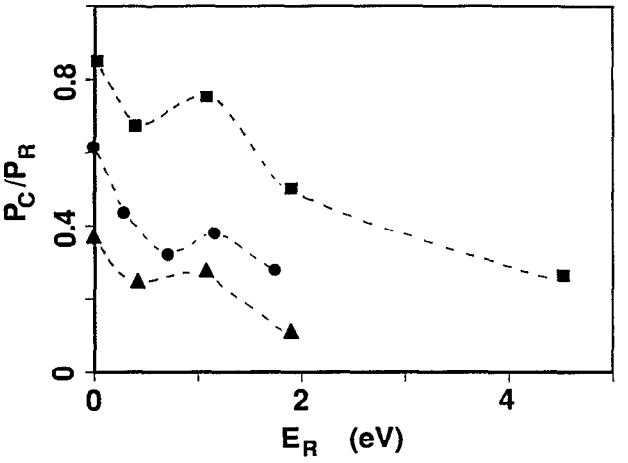

FIG. 16. Summary of the branching ratios (P_C/P_R) plotted vs relative translational energy between the reactants (E_R), for the reaction $[Na_4Cl_3]^+Ar_{12} + Cl^-$, for three initial vibrational temperatures of the reactant cluster: $T^0_{vib} = 31.6$, 189, and 316 K denoted by filled squares, circles, and triangles, respectively. The dashed lines are drawn to guide the eye. Energy in eV.

(e) All associative reactions involve the release of Ar atoms, almost all in the form of monomers. The number of ejected Ar atoms depends on the size of the reactant clusters and the reaction conditions.

(f) Studies of the dynamics of the associative reactions reveal that the major part of the energy release occurs in the very initial stage of the collision, resulting in the ejection of one or two translationally hot Ar monomers. The amount of energy carried by these initially ejected Ar atoms, determines the reaction path; i.e., a larger energy loss at the initial stage of the reaction is more likely to result in a product with a ground state isomeric structure.

In this context we remark that in all our calculations the simulated trajectories were of 25 ps in duration. Test runs, where the simulations were continued to the nanosecond range, show that typically about two additional Ar atoms were evaporated, resulting in further small cooling of the product cluster. However, in no case did the structure of the product alkali-halide cluster change from that obtained already in the 25 ps simulations. Evidently, the internal temperatures of the product clusters are below the temperature range for transitions between the isomeric forms (see Fig. 1). Coupled with the fact that the transformations between isomeric forms involve activation barriers (e.g., estimated to be of the order of 0.5 eV for the transformation between the cubic and ring isomers of Na_4Cl_4),[14(a)] the reaction prod-

ucts remain in the isomeric structures which they assume at the early stages of the reaction process.

At this point we wish to propose that for a given initial vibrational temperature the observed trend of overall decrease in the branching ratio P_C/P_R with increasing relative translational energy (E_R) between the reactants (see Fig. 16), originates from combined energetic and geometric considerations of the collision process. As the incident anion approaches the positively charged cluster from the initial separation, it accelerates, gaining an energy $E_{\text{coul}} \simeq 2$ eV (in addition to E_R) just before the first collision (thus the energy of the ion as it impacts the cluster is $E'_R = E_R + E_{\text{coul}}$. Even when $E_R = 0$, the anion impacts the cluster with a significant energy compared to the typical binding energies of Ar atoms to the cluster, i.e., about 0.3–0.4 eV.

The probability for ejection of an energetic (translationally hot) Ar atom at the very initial stage of the collision process involves two factors: (i) Transfer of energy from the incident anion to the system; and (ii) ejection (escape) of the Ar atom from the cluster. As aforementioned, the reaction path (i.e., branching ratio of the product's isomeric form) is determined by the amount of energy transferred in the initial collision stage (see Figs. 6 and 7). We also noted that the decreasing trend in P_C/P_R vs E_R (Fig. 16) correlates with an overall decrease in the probability for generating products of the cube isomer form (P_C). Moreover, we observe that for a given initial temperature (T^0_{vib}) of the reactant cluster the properties (i.e., vibrational energy, potential energy, and number of remaining attached Ar atoms) of the cube-isomer products are rather insensitive to the initial relative translational energy (E_R) between the reactants [see Tables I(a)–I(c)]. Consequently, in the following we focus on the factors which determine P_C.

First we consider the dependence of the energy transfer from the incident ion to the cluster. We note from plots of the energy of Ar monomers in the reaction resulting in cube-isomer products (see bottom of Fig. 6 for the case of the initial $[Na_4Cl_3]^+Ar_{12}$ cluster at 31.6 K, with similar results obtained for other initial temperatures) that the kinetic energy of the first ejected Ar atom (or two atoms) grows approximately linearly with E_R in such a way that the translational energy of the Cl^- ion after that initial collision is approximately the same (denoted by ϵ_c) independent of the ion initial relative kinetic energy (E_R). In other words, in order to favor products in the cube-isomer form, the amount of energy loss ΔE by the Cl^- in the initial collision (i.e., the energy imparted to the Ar atom) should be such that $\Delta E \geqslant E_R - \epsilon_c$.

For the purpose of our discussion we model the binary collision of the Cl^- anion with an Ar atom using hard-sphere collision theory,[16] where the fractional energy loss $\Delta(\theta) = \Delta E/E'_R$ in a collision between a stationary target particle of mass M (Ar in our case) and an incident particle of mass m (i.e., Cl^-) with a kinetic energy E'_R, is given by

$$\Delta(\theta) = 4\frac{M}{m}\left(\frac{m}{m+M}\right)^2 \cos^2\theta \equiv \kappa \cos^2\theta, \tag{3}$$

where θ is the scattering angle of the target particle ($\theta = 0$ corresponds to a head-on collision) and for our case $\kappa = 0.996$. Based on the previous discussion we assume a constant critical value (ϵ_c) for the energy of the Cl^- ion after the first collision with an Ar atom. Integrating over all scattering angles θ, which lead to an energy loss $\Delta \equiv \Delta E/E'_R \geqslant (E'_R - \epsilon_c)/E'_R \equiv \Delta_c$, we find for the probability of such events

$$P_{\text{coll}}(\Delta \geqslant \Delta_c) = \int_0^{\theta_c} p(\theta)d\theta = \int_0^{\theta_c} \sin(2\theta)d\theta = \sin^2\theta_c, \tag{4}$$

where $\cos^2\theta_c = \Delta_c/\kappa$. Thus we find that

$$P_{\text{coll}}(\Delta \geqslant \Delta_c) = 1 - \frac{1}{\kappa} + \frac{\epsilon_c}{\kappa E'_R}, \tag{5}$$

exhibiting the expected decreasing behavior as a function of E'_R (and thus E_R), in correspondence with the overall trend in Fig. 16.

The geometric considerations pertain to the other characteristic features exhibited in the plots of the branching ratio vs incident energy for given initial temperature, i.e., the maxima in cube-isomer production observed at $E_R \sim 1$–1.2 eV (see Fig. 16). This effect may be attributed to the enhancement of *direct ejection* of the Ar atom energized by collision with the incident Cl^- ion. (In this context we would like to remind that trajectories favoring cube-isomer products correspond to the ejection of translationally hot Ar monomers at the initial stage of the reaction.) We associate this enhancement with an increase in the effective mean impact radius (r_a) of the incoming Cl^- with respect to the cluster upon the first collision. We define r_a as the distance of the Cl^- ion from the center of mass of the cluster, perpendicular to the velocity of the ion [see Fig. 17(a)]. As the relative kinetic energy between the reactants (E_R) is increased the mean value of r_a will grow[16] leading to collisions of the Cl^- ion with Ar atoms located at the edge of the cluster [see Fig. 17(a)] for which a larger sector of scattering angles corresponds to ejection of Ar monomers without secondary (or multiple) collisions. We suggest that the enhancement of the direct monomer ejection channel at $E_R \sim 1$ eV is portrayed by the local maximum probability for reactions leading to cube-isomer products (Fig. 16). (It is interesting to note here that we have observed that trajectories with large initial impact parameter, $r_I \sim 8$ Å, and for initial energy $E_R \sim 1.0$ eV, result in glancing collisions.) For larger values of E_R the decreasing trend given by Eq. (5), dominates, leading to the monotonic decrease seen in Fig. 16.

As seen from our results, for the systems that we have investigated (i.e., alkali-halide clusters embedded in argon), it is possible to "tune" the branching ratio between the reaction products (i.e., modify the relative probabilities for the different product isomers) by varying the reaction parameters (initial vibrational temperature of the reactants and relative translational energy between the collision partners) and/or number of embedding Ar atoms. However, the nature and relative strengths of the interactions in our system (i.e., ion–ion, Ar–ion, and Ar–Ar) and the magnitude of barriers for interconversion between the reaction products (i.e., isomerization barriers) set a limit to the degree of annealing which can be achieved. Thus the fast nonstatistical

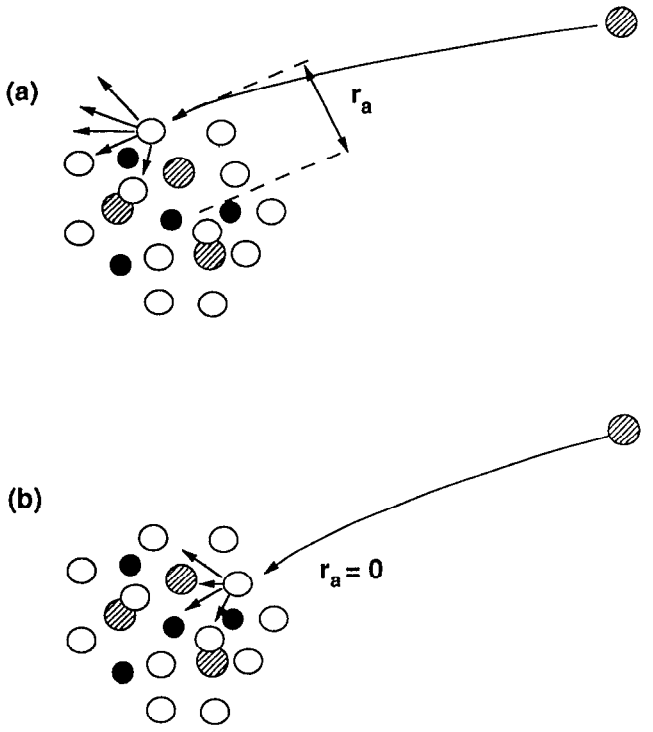

FIG. 17. Schematics of collision processes illustrating events favoring direct ejection of an energized monomer after the initial collision between the incident ion and the cluster [in (a)], and those resulting in multiple collisions of the energized Ar atom [in (b)]. The definition of the effective impact radius, r_a, is shown in (a). Filled and dashed circles represent Na^+ and Cl^- ions, respectively, and the Ar atoms are represented by empty circles.

cooling of the associated (compound) cluster in the initial reaction stage (via transfer of energy leading to the release of one or two hot Ar atoms) traps the reaction products in the different channels (i.e., different isomeric forms). Further cooling past the initial stage occurs at a very slow rate, because of the relatively strong Ar–ion interactions, and thus is ineffective in inducing structural transformations and further annealing of the products toward the ground state isomeric form.

Nevertheless, consideration of larger Ar environments, as well as different reactants and/or embedding cluster environments, coupled with appropriate selection of collision parameters, may enable optimal control of reaction pathways and product branching ratios.

Another class of cluster catalyzed reactions which we propose, is the collision between clusters, in which reactants are embedded, under conditions which result in the initiation of a shock wave in the intermediate compound cluster. (Similar conditions may be also achieved by colliding clusters with solid surfaces.) This would lead to transient local pressure and temperature shock conditions which may induce processes such as dissociation or vibrational (and perhaps even electronic) excitations, which, in turn, may lead to subsequent reactions, with the cluster environment serving as a local heat bath.

ACKNOWLEDGMENTS

This research is supported by the U.S. Department of Energy (DOE) under Grant No. FG05-86ER45234. We thank Professor Flannery and Professor McDaniel for useful discussions of gas-phase ion–ion recombination processes. H.-P.K. gratefully acknowledges partial support by the Foundation of Neste Corporation, the Wihuri Foundation, and the Finnish Academy of Sciences. Calculations were performed at the National Energy Research Supercomputer Center, Livermore, California, through a computer-time grant by DOE.

[1] See articles in (a) *Atomic and Molecular Clusters*, edited by E. R. Bernstein (Elsevier, Amsterdam, 1990); (b) *Atomic and Molecular Beam Methods*, edited by G. Scoles (Oxford University, London, 1989); (c) *Elemental and Molecular Clusters*, edited by G. Benedek, T. P. Martin, and G. Paccioni (Springer, Berlin, 1989).

[2] See reviews in (a) U. Landman in *Computer Simulation Studies in Condensed Matter Physics*, edited by D. P. Landau, K. K. Mon and H.-B. Schuttler, (Springer, Berlin, 1988); (b) R. S. Berry, T. L. Beck, H. L. Davis, and J. Jellinek, Adv. Chem. Phys. **70**, 75 (1988).

[3] (a) U. Landman in Ref. 2(a), p. 144; (b) J. Jortner, D. Scharf, and U. Landman in Ref. 1(c), p. 148. (c) R. N. Barnett, U. Landman, G. Rajagopal, and A. Nitzan, Isr. J. Chem. **30**, 85 (1990); (d) D. L. Freeman and J. D. Doll, Adv. Chem. Phys. **70**, 139 (1988); (e) C. L. Cleveland and U. Landman, Phys. Rev. B **39**, 117 (1989).

[4] For representative experimental studies see (a) J. L. Elkind, F. D. Weiss, J. M. Alford, R. T. Laaksonen, and R. E. Smalley, J. Chem. Phys. **88**, 5215 (1988); (b) W. D. Reents, Jr. and M. L. Mandich, J. Phys. Chem. **92**, 2908 (1988); (c) W. F. Hoffman, E. K. Parks, and S. J. Riley, J. Chem. Phys. **90**, 1526 (1989); (d) Y. M. Hamrick and M. D. Morse, J. Phys. Chem. **93**, 6494 (1989); (e) S. K. Loh, L. Lian, and P. B. Armentrout, J. Chem. Phys. **91**, 6148 (1989); (f) P. Fayet, A. Kaldor, and D. M. Cox, *ibid.* **92**, 254 (1990); (g) K. M. Creegan and M. F. Jarrold, J. Am. Chem. Soc. **112**, 3768 (1990); R. E. Leuchtner, A. C. Harms, and A. W. Castlemen, Jr., J. Chem. Phys. **92**, 6527 (1990); **91**, 2753 (1989).

[5] For representative theoretical studies see (a) K. Raghavan, M. S. Stave, and A. E. DePristo, J. Chem. Phys. **91**, 1904 (1989); (b) J. E. Adams, *ibid.* **92**, 1849 (1990); (c) J. Jellinek and Z. B. Guvenc, Z. Phys. D (in press).

[6] H. W. Ellis, R. Y. Pai, I. R. Gatland, E. W. McDaniel, R. Wernlund, and M. J. Cohen, J. Chem. Phys. **64**, 3935 (1976).

[7] B. D. Kay, V. Herman, and A. W. Castleman, Jr., Chem. Phys. Lett. **80**, 469 (1981).

[8] M. R. Flannery and E. J. Mansky, J. Chem. Phys. **88**, 4228 (1988).

[9] M. R. Flannery, in *Molecular Processes in Space*, edited by T. Watanabe, I. Shimamura, M. Shimizu, and Y. Itikawa (Plenum, New York, 1990), p. 145.

[10] M. Born and K. Huang, *Dynamical Theory of Crystal Lattices* (Oxford University, London, 1954).

[11] R. Ahlrichs, H. J. Bohm, S. Brode, K. T. Tang, and J. P. Toennies, J. Chem. Phys. **88**, 6290 (1988).

[12] M. P. Allen and D. J. Tildesley, *Computer Simulation of Liquids* (Clarendon, Oxford, 1987).

[13] J. R. Fox and H. C. Andersen, J. Phys. Chem. **88**, 4019 (1984).

[14] (a) T. P. Martin, Phys. Rep. **95**, 167 (1983); (b) E. C. Honea, M. L. Homer, P. Labastie, and R. L. Whetten, Phys. Rev. Lett. **63**, 394 (1989); (c) J. Luo, U. Landman, and J. Jortner, in *Physics and Chemistry of Small Clusters*, edited by P. Jena, B. K. Rao and S. N. Khanna (Plenum, New York, 1987), p. 201.

[15] R. D. Levine and R. B. Bernstein, *Molecular Reaction Dynamics and Chemical Reactivity* (Oxford University, Oxford, 1987).

[16] E. W. McDaniel, *Atomic Collisions* (Wiley, New York, 1980).